

Effects of Mechanical Damage and Temperature on the Electrical Performance of CIGS Thin-Film Solar Cells

Hansung Kim , Member, IEEE, and Benjamin G. Wojkovich

Abstract—In this paper, we investigate the effect of mechanical damage and temperature on copper indium gallium diselenide (CIGS) thin-film solar cells through experiments and modeling. After generating mechanical damage on CIGS solar cell with 20% increments, the electrical performance was measured (current-voltage curve) while temperature was varying from 10 to 70 °C at 20° increments. Other measured values are open-circuit voltage (V_{oc}), fill factor (ff), maximum power (P_{max}). Those electrical values (V_{oc} , ff, P_{max}) are found as a function of temperature and percent damage. Moreover, the parameters of the single diode solar cell model were obtained as a function of temperature and percentage damage: light generation current (I_L), saturation current (I_0), shunt resistance (R_{sh}), and series resistance (R_s). Our paper contributes to the deeper understanding of the concurrent effect of temperature and mechanical damage to solar cells.

Index Terms—Copper indium gallium diselenide (CIGS), electrical performance, mechanical damage, temperature, thin-film solar cells.

I. INTRODUCTION

COPPER indium gallium diselenide (CIGS) solar cells are one of the most widely used thin-film solar cells. Since these thin-film solar cells are flexible, they are installed on the roof of a house as shingles or on the roof of a vehicle as solar roof. Several car companies (Audi, Toyota, and Tesla) announced their plans for electric vehicles with solar roofs. In the United States, an average of 1250 tornadoes and 6 hurricanes are reported every year [1], [2]. Therefore, reliability evaluation of solar cells due to mechanical damages caused by tornadoes and hurricanes is very desirable. Moreover, the evaluation of temperature effect on solar cells is critical to accurately predict the solar cell performance. Since flexible solar cells are generally thin, variation of cell temperature due to environmental temperature is quite rapid compared with conventional silicon solar cells.

Manuscript received February 26, 2018; revised May 13, 2018 and July 14, 2018; accepted July 17, 2018. Date of publication August 6, 2018; date of current version August 20, 2018. This work was supported in part by Purdue PRF Faculty Research grant and in part by research grant from College of ES of Purdue University Northwest. (Corresponding author: Hansung Kim.)

The authors are with Purdue University Northwest, Hammond, IN 46323-2094 USA (e-mail: kim886@purdue.edu; bwojkovi@pnw.edu).

Color versions of one or more of the figures in this paper are available online at <http://ieeexplore.ieee.org>.

Digital Object Identifier 10.1109/JPHOTOV.2018.2858557

In this paper, we concurrently evaluate the effect of temperature and mechanical damage on CIGS solar cells to answer the following critical questions.

- 1) Does the mechanical damage alter the temperature effect on solar cells?
 - a) For example, does an undamaged solar cell at 20 °C have the same open-circuit voltage as a 20% damaged cell at 20 °C? How the damage effect be quantified?
- 2) Does the temperature alter the mechanical damage effect on solar cells?
 - a) For example, does a solar cell with 10% damage at 10 °C have the same open-circuit voltage as a solar cell with 10% damage at 70 °C? How can this be quantified?

The percentage of damage is based on the damaged area compared with the total area of the CIGS solar cell, which represents the percentage of mechanically separated regions in the solar cell. In this study, we mimic the damage caused by tornadoes or hurricanes by inflicting the damage through drimmel tool.

For conventional silicon solar cells, the mechanical damage presents as crack damage. There are multiple studies on the crack effect on the solar cell performance. Pletzer *et al.* [3] presented the analysis of the influence of cracks on the electrical parameters of silicon solar cells using a two-diode model. The analysis clearly shows that cracks mainly affect the recombination current density, which results in the decrease of fill factor (ff) as well as efficiency. Sera [4] developed a method to detect the failure of silicon solar panel by monitoring the panel's series resistance based on a single-diode model. The increase of series resistance is closely related to the degradation of PV systems [5]–[7]. Wang *et al.* [5] found that series resistance (R_s) increases and current source (I_L) decreases when a solar panel contains cracks. Those parameters are based on the single-diode model of solar cells. Kontges *et al.* [8] also reported that when an inactive cell area of silicon solar cells is between 12% and 50%, the power loss in the PV module is linearly proportional to the area of inactive cells. However, most studies investigating the crack (mechanical) damage effect are based on silicon solar cells. There are few studies on the mechanical damage effect on flexible thin-film solar cells. However, there are some previous studies on the effect of bending and rolling on the CIGS solar cells. Chirila *et al.* [9] performed stress tests comprised of more than 1000 cycles of rolling and unrolling of CIGS solar

cells grown on flexible polymer films using a cylinder with a 2 cm radius. They reported that the degradation after the stress test was about 4%. Wiedeman [10] performed bending tests of CIGS solar cells around a mandrel to determine the bend radius generating significant damage. Cells were examined in both compressive (grid toward mandrel) and tensile (grid away from mandrel) stress. He reported that compressive stress generates more damage than tensile stress, and the bend radius more than 0.25 inch starts to generate significant damage to the performance of CIGS solar cells. Lee *et al.* [11] also performed bending tests of Pbs/Cds thin-film solar cells by applying a load between two parallel holders. They illustrated the efficiency versus bending strain curve in the paper. They also mentioned that the value of the short-circuit current is significantly reduced above a certain bending strain, while open-circuit voltage is not much influenced by the bending strain.

There are also numerous studies of temperature effect on the electrical performance of solar cells. Skoplaki and Palyvos [12] reviewed numerous existing models relating efficiency and power of solar cells with temperature. They concluded that both electrical efficiency and power output of the PV module has an inversely linear relationship with cell operating temperature. Based on the semiconductor theory, it can be reasoned that open-circuit voltage, ff , and maximum power decreases as the temperature increases. However, there are few studies of temperature effect taking into account the mechanical damage severity.

Therefore, in this paper, we systematically investigate the effect of temperature and mechanical damage simultaneously with 20 °C temperature increments ranging from 10 to 70 °C along with 20% increments of damage ranging from 0% to 80%. Through this research, several significant trends were discovered or confirmed for CIGS thin-film solar cells as detailed below.

- 1) Temperature effect is more significant at lower damage levels for efficiency and maximum power.
- 2) With larger than 60% damage, the efficiency and maximum power remain constant regardless of temperature.
- 3) Resistance of solar cell increases as the damage level increases.
- 4) Resistance of solar cell decreases as the temperature increases.

There are numerous existing methods to determine the mechanical (crack) damage in the solar cells such as electroluminescence (EL) [3], [13], [14], resonance ultrasonic vibration (RUV) [15], [16], photoluminescence [17], infrared [18], [19]. In this paper, the percentage of the damaged area in CIGS solar cells was measured using an infrared camera and postprocessing. Image-J software was used for postprocessing of infrared images of damaged CIGS solar cells [20].

II. METHOD

A. Experimental Procedure

The CIGS solar cell used for this paper is FG-SM12-11 from Global Solar Company. This flexible thin-film solar cell is designed for Portable Solar Charger products. Fig. 1 shows the in-house temperature-controlled environmental chamber for the

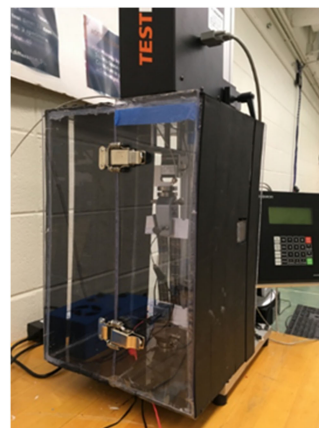


Fig. 1. In-house temperature-controlled environmental chamber.

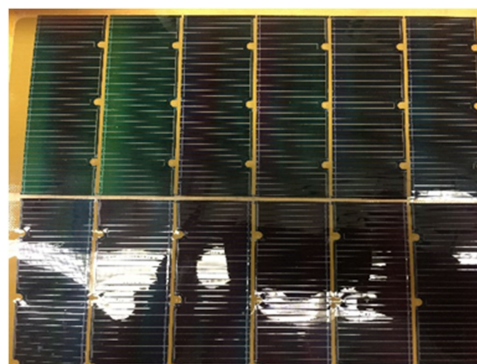


Fig. 2. FG-SM12-11 CIGS thin-film solar cell.

solar cell experiment, and Fig. 2 shows FG-SM12-11 CIGS thin-film solar cell.

For our experiment, the CIGS thin film is placed in the temperature-controlled chamber, then standard solar cell testing procedures are applied with 1000 W/m² light incident. Before running the experiment, the temperature was maintained at a constant value. Temperature was measured *in situ* while running the experiments. There was a change in temperature between the beginning and the end of each experiment, which was about 2–4 °C. We used average value for the temperature measurement.

However, since we used a tungsten halogen lamp instead of a highly rated solar simulator as a continuous light source and some light spectrum might be reflected by the environmental chamber, the measured efficiency was lower than the value that the manufacturing company claims. The main goal of this study is to investigate how temperature and mechanical damage affect the solar cell performance qualitatively instead of quantitatively. If highly rated solar simulators were used, the quantitative values of the results would be different. However, we believe that similar qualitative results would be obtained as long as similar types of CIGS solar cell are used.

Mechanical damage was generated ranging from 0% to 80% with a 20% increment using a drimmel tool. The damaged area was measured using ImageJ software based on the infrared pictures which were taken after applying a biasing voltage. Fig. 3

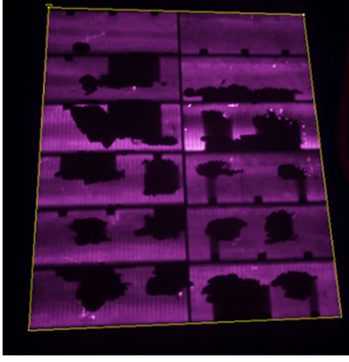


Fig. 3. Infrared image of damaged cell. Black color represents the damaged region. Total area (yellow rectangle) is measured in pixels.

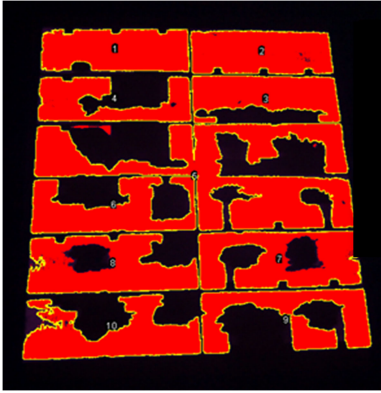


Fig. 4. Image after postprocessing. Red color represents the undamaged area. Black color represents the damaged region. Area of each undamaged region is shown in the table.

shows the infrared image of a damaged cell, where black color displays the damaged region. Fig. 4 illustrates the cell image after the postprocessing by ImageJ software. Red color represents the undamaged area, while black color represents the damaged one. Finally, the cell is connected to the solar analyzer which measures its current–voltage (I – V) curve at a specific percent damage and temperature.

B. Modeling Procedure

A single-diode circuit is used to model our CIGS solar cell (see Fig. 5), which is composed of light generation current (I_L), saturation current (I_0), shunt resistance (R_{sh}), and series resistance (R_s).

The equation that describes the solar cell circuit shown in Fig. 5 is as follows:

$$I = I_L - I_0 \left\{ \exp \left[\frac{(V + IR_s)}{nV_t} \right] - 1 \right\} - \frac{(V + IR_s)}{R_{sh}} \quad (1)$$

where n is the ideal factor. The thermal voltage (V_t) depends on the temperature (T) of the solar cell, in Kelvin, and the Boltzmann constant (K) and elementary charge (q)

$$V_t = \frac{k \times T}{q}. \quad (2)$$

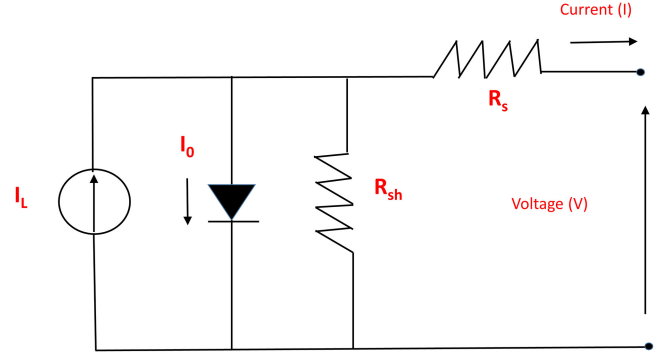


Fig. 5. Single diode model of solar cell [6].

Based on the collected experimental data, MATLAB software was used to find the parameters of a single-diode solar cell model (I_L , I_0 , R_{sh} , R_s) as a function of percent damage and temperature. MATLAB software uses an unconstrained nonlinear optimization technique based on the simplex search method of Lagarias *et al.* [21]. In order to observe the variation of parameters as a function of percent damage and temperature, the ideal factor was fixed to be 1.5. Initial values of parameters in the single-diode solar model (I_L , I_0 , R_{sh} , R_s) are calculated as detailed below.

- 1) The short-circuit current (I_{sc}) is used as the initial value of light-generated current (I_L) for optimizing I_L

$$I_L = I_{sc}. \quad (3)$$

- 2) The diode reverse saturation current can be found using the solar cell's light-generated current, open-circuit voltage, and ideality factor

$$I_0 = \frac{I_L}{\exp \left[\frac{V_{oc}}{(0.025 \times n)} \right] - 1}. \quad (4)$$

- 3) The shunt resistance is the inverse slope of the I – V curve at current short circuit

$$R_{sh} = \frac{-dV}{dI} @ I_{sc}. \quad (5)$$

- 4) Series resistance is the inverse slope of the I – V curve at voltage open circuit

$$R_s = \frac{-dV}{dI} @ V_{oc}. \quad (6)$$

III. RESULTS AND DISCUSSION

Fig. 6 shows the open-circuit voltage as a function of damage and temperature. When the damage is less than $\sim 60\%$, the open-circuit voltage (V_{oc}) decreases as the damage increases. However, with 60% or more damage, V_{oc} remains constant even though the damage increases indicating the active operation of the bypass diode. Moreover, Fig. 6 illustrates that V_{oc} decreases as the temperature increases. Fig. 7 shows the behavior of the ff as a function of damage and temperature. Similar to V_{oc} , the overall value of the ff decreases as the damage increases. However, there is an unexpected increase of ff, around 80% damage, due to the operation of the bypass diode.

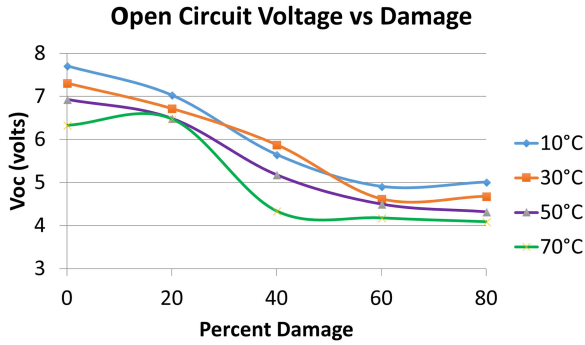


Fig. 6. Open-circuit voltage (V_{oc}) as a function of damage and temperature.

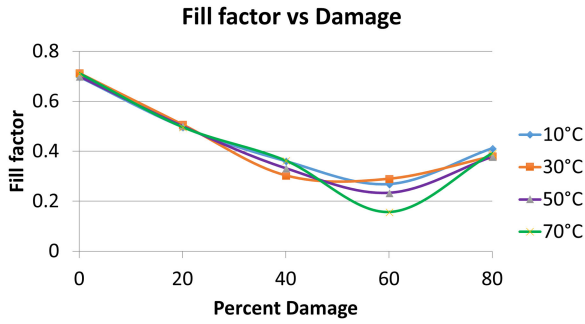


Fig. 7. Fill factor (ff) as a function of damage and temperature.

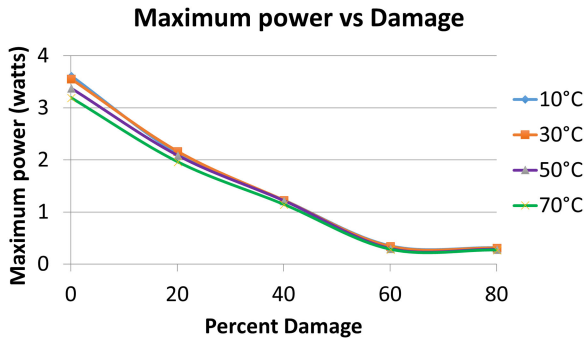


Fig. 8. Maximum power (P_{max}) as a function of damage and temperature.

Fig. 8 shows the maximum power (P_{max}) as a function of damage and temperature. Similar to V_{oc} , P_{max} decreases as the damage increases up to 60% and remains constant at higher damage. Also higher P_{max} is achieved when the temperature is lower. Efficiency is also found to have the same trend as P_{max} .

Based on the MATLAB simulation of unconstrained optimization, parameters of the single diode circuit model were obtained as a function of temperature and percent damage: light generation current (I_L), saturation current (I_0), shunt resistance (R_{sh}), and series resistance (R_s).

Fig. 9 illustrates the magnitude of shunt resistance as a function of damage and temperature. It is observed that the shunt resistance decreases (R_{sh}) as the damage increases. It is also found that the shunt resistance decreases as the temperature increases. Generally, the shunt resistance is inversely related to the magnitude of the defect in the solar cell. Lower shunt resistance provides an alternative current path for the light-generated

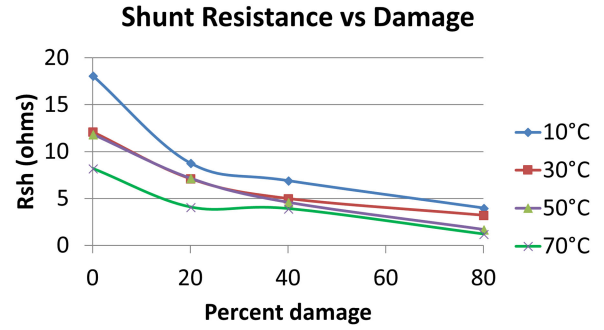


Fig. 9. Shunt resistance (R_{sh}) as a function of damage and temperature.

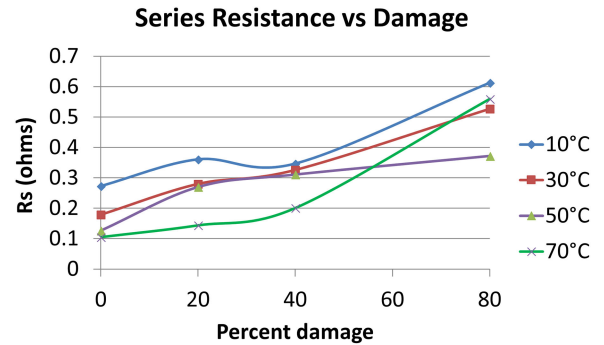


Fig. 10. Series resistance (R_s) as a function of damage and temperature.

current, causing the reduction of current flowing through the solar cell junction as shown in Fig. 5, which eventually leads to the reduction of power and efficiency [22].

Series resistance impacts the ff of solar cells resulting in decreased efficiency [22]. Fig. 10 illustrates the magnitude of series resistance as a function of damage and temperature. It is observed that the series resistance increases as the damage increases like the case of silicon solar cells [4]–[6]. It is also found that the series resistance decreases as the temperature increases similar to the shunt resistance. Series resistance differs from shunt resistance because a low value of series resistance is desired for optimal solar cell operation, contrary to the shunt resistance.

There are several complex phenomena taking place in the damaged module such as cell mismatch, hot spot, and the operation of bypass-diode. Identifying individual effects of cell mismatch and hot spot on solar cell performance is beyond our scope. However, we believe that the lumped (combined) effect of mismatch and hot spot is incorporated into model parameters (series resistance and shunt resistance). We assume that the increase of external damage is proportional to the increase of cell mismatch and hot spot in the module, resulting in the degradation of solar cell performance. The degradation of solar cell is manifested with the increase of R_s and decrease of R_{sh} in the diode model.

Fig. 11 shows the behavior of the light generation current (I_L) as a function of damage and temperature. The overall value of the light-generated current (I_L) decreases with the increase in damage as well as the decrease in temperature. However, there is an unexpected increase of I_L , around 40% damage, which is due

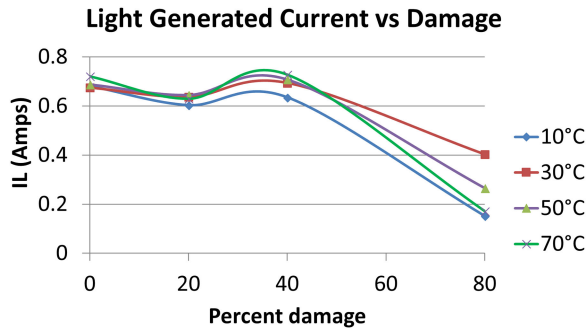


Fig. 11. Light-generated current (I_L) as a function of damage and temperature.

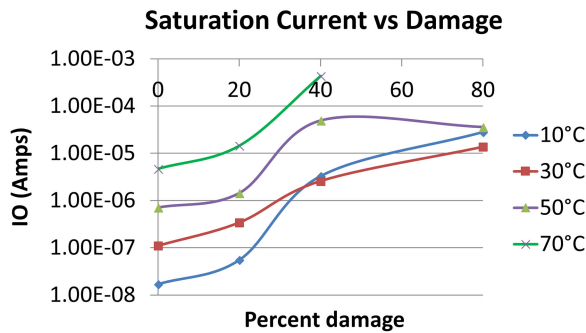


Fig. 12. Saturation current (I_0) as a function of damage and temperature.

to the bypass diode. Even though the short-circuit current (I_{sc}) is generally the same as I_L , in the case of high series resistance, I_{sc} is less than I_L [22]. Since the R_s increases $\sim 200\%$ – $\sim 600\%$ as the damage increases in our study, I_L cannot be the same as I_{sc} in the case of high resistance. The experimentally obtained I_{sc} is used as the initial value of I_L to accurately find the I_L .

The last parameter of the single diode model obtained by MATLAB optimization is the reverse saturation current (I_0). The saturation current is the amount of current leakage due to the recombination in a device. Larger recombination in diodes is attributed to an increase in saturation current. For the p-n junction of the solar cell to be able to collect the light-generated current, the saturation current should be at a minimal value. Since the magnitude of the saturation current is between the order of 10^{-8} and 10^{-4} , the logarithmic scale is used to identify the trend of I_0 clearly. Fig. 12 shows an increase in saturation current at higher temperatures and damage. This increase caused the p-n junctions of the solar modules inefficiently collect the light carriers.

It is possible that metastable (transient) behavior due to light soaking would skew experimental results [23]–[25]. However, investigating the effect of light soaking was beyond our scope, which could complicate our experimental and modeling procedures.

IV. CONCLUSION

We investigated that the effects of mechanical damage and temperature on the electrical performance of CIGS thin-film solar cells. Through experiment, we observed that open-circuit

voltage and efficiency decrease with the increasing damage and temperature. The short-circuit current decreases with the increasing damage and decreasing temperature. The effect of damage on the electrical performance is more significant at lower temperatures. Also, the effect of temperature on the electrical performance is more significant at a lower percentage damage. Based on the unconstrained MATLAB optimization, the parameters of a single diode solar cell model were obtained as a function of temperature and percentage damage: light generation current (I_L), saturation current (I_0), shunt resistance (R_{sh}), and series resistance (R_s). The light generation current (I_L) decreases with the increasing damage and decreasing temperature. The saturation current (I_0) decreases with the decreasing damage and decreasing temperature. The shunt resistance (R_{sh}) decreases with the increasing damage and increasing temperature. The series resistance (R_s) decreases with the decreasing damage and increasing temperature.

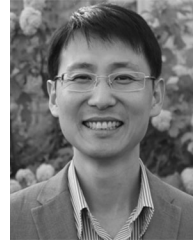
ACKNOWLEDGMENT

Authors appreciate fundings from Purdue PRF Faculty Research grant as well as research grant from College of ES of Purdue University Northwest.

REFERENCES

- [1] N. O. A. Administration, *U.S. Tornado Climatology*, Jul. 2018. [Online]. Available: <https://www.ncdc.noaa.gov/climate-information/extreme-events/us-tornado-climatology>
- [2] N. O. A. Administration, "How many tropical cyclones have there been each year in the Atlantic basin?", 2018. [Online]. Available: <http://www.aoml.noaa.gov/hrd/tcfaq/E11.html>
- [3] T. M. Pletzer, J. I. van Molken, S. Rilssand, O. Breitenstein, and J. Knoch, "Influence of cracks on the local current-voltage parameters of silicon solar cells," *Prog. Photovolt.*, vol. 23, no. 4, pp. 428–436, Apr. 2015.
- [4] D. Sera, "Series resistance monitoring for photovoltaic modules in the vicinity of MPP," in *Proc. 25th Eur. Photovolt. Sol. Energy Conf. Exhibi.*, Valencia, Spain, Sep. 2010, pp. 4506–4510.
- [5] W. G. Wang *et al.*, "Fault diagnosis of photovoltaic panels using dynamic current-voltage characteristics," *IEEE Trans. Power Electron.*, vol. 31, no. 2, pp. 1588–1599, Feb. 2016.
- [6] S. Spataru, D. Sera, T. Kerekes, and R. Teodorescu, "Diagnostic method for photovoltaic systems based on light I-V measurements," *Sol. Energy*, vol. 119, pp. 29–44, Sep. 2015.
- [7] D. Sera, R. Teodorescu, and P. Rodriguez, "Photovoltaic module diagnostics by series resistance monitoring and temperature and rated power estimation," in *Proc. 34th Annu. Conf. IEEE Ind. Electron. Soc.*, 2008, pp. 2195–2199.
- [8] M. Kontges, I. Kunze, S. Kajari-Schroder, X. Breitenmoser, and B. Bjorneklett, "The risk of power loss in crystalline silicon based photovoltaic modules due to micro-cracks," *Sol. Energy Mater. Sol. Cells*, vol. 95, no. 4, pp. 1131–1137, Apr. 2011.
- [9] A. Chirila *et al.*, "Highly efficient Cu(In,Ga)Se-2 solar cells grown on flexible polymer films," *Nature Mater.*, vol. 10, no. 11, pp. 857–861, Nov. 2011.
- [10] S. Wiedeman, "Cost and reliability improvement for CIGS-based PV on flexible substrate," Nat. Renewable Energy Lab., Golden, CO, USA, NREL/SR-520-45213, 2011.
- [11] S. M. Lee, D. H. Yeon, B. C. Mohanty, and Y. S. Cho, "Tensile stress-dependent fracture behavior and its influences on photovoltaic characteristics in flexible PbS/CdS Thin-film solar cells," *ACS Appl. Mater. Interfaces*, vol. 7, no. 8, pp. 4573–4578, Mar. 2015.
- [12] E. Skoplaki and J. A. Palyvos, "On the temperature dependence of photovoltaic module electrical performance: A review of efficiency/power correlations," *Sol. Energy*, vol. 83, no. 5, pp. 614–624, May 2009.
- [13] A. Morlier, F. Haase, and M. Kontges, "Impact of cracks in multicrystalline silicon solar cells on PV module power—a simulation study based on field data," *IEEE J. Photovolt.*, vol. 5, no. 6, pp. 1735–1741, Nov. 2015.

- [14] M. Sander, S. Dietrich, M. Pander, M. Ebert, and J. Bagdahn, "Systematic investigation of cracks in encapsulated solar cells after mechanical loading," *Sol. Energy Mater. Sol. Cells*, vol. 111, pp. 82–89, Apr. 2013.
- [15] A. Belyaev, O. Polupan, W. Dallas, S. Ostapenko, D. Hess, and J. Wohlgenuth, "Crack detection and analyses using resonance ultrasonic vibrations in full-size crystalline silicon wafers," *Appl. Phys. Lett.*, vol. 88, no. 11, 2006, Art. no. 111907.
- [16] W. Dallas, O. Polupan, and S. Ostapenko, "Resonance ultrasonic vibrations for crack detection in photovoltaic silicon wafers," *Meas. Sci. Technol.*, vol. 18, no. 3, pp. 852–858, Mar. 2007.
- [17] M. Demant *et al.*, "Detection and analysis of micro-cracks in multi-crystalline silicon wafers during solar cell production," in *Proc. 37th IEEE Photovolt. Spec. Conf.*, Seattle, WA, USA, Jun. 2011, pp. 001641–001646.
- [18] W. S. M. Brooks, D. A. Lamb, and S. J. C. Irvine, "IR reflectance imaging for crystalline Si solar cell crack detection," *IEEE J. Photovolt.*, vol. 5, no. 5, pp. 1271–1275, Sep. 2015.
- [19] E. D. Dunlop and D. Halton, "Radiometric pulse and thermal imaging methods for the detection of physical defects in solar cells and Si wafers in a production environment," *Sol. Energy Mater. Sol. Cells*, vol. 82, no. 3, pp. 467–480, May 2004.
- [20] C. A. Schneider, W. S. Rasband, and K. W. Eliceiri, "NIH image to imageJ: 25 years of image analysis," *Nature Methods*, vol. 9, no. 7, pp. 671–675, Jul. 2012.
- [21] J. C. Lagarias, J. A. Reeds, M. H. Wright, and P. E. Wright, "Convergence properties of the Nelder-Mead simplex method in low dimensions," *SIAM J. Optim.*, vol. 9, no. 1, pp. 112–147, Dec. 1998.
- [22] C. Honsberg and S. Bowden, PV Education.org. 2018. [Online]. Available: <http://www.pveducation.org/>
- [23] T. Walter, "Reliability issues of CIGS-based thin film solar cells," *Adv. Photovolt.*, vol. 92, pp. 111–150, 2015.
- [24] M. G. Deceglie, T. J. Silverman, B. Marion, and S. R. Kurtz, "Metastable changes to the temperature coefficients of thin-film photovoltaic modules," in *Proc. IEEE 40th Photovolt. Spec. Conf.*, 2014, pp. 337–340.
- [25] M. G. Deceglie *et al.*, "Validated method for repeatable power measurement of CIGS modules exhibiting light-induced metastabilities," *IEEE J. Photovolt.*, vol. 5, no. 2, pp. 607–612, Mar. 2015.



Hansung Kim (M'16) received the M.S. degree in dynamic battery modeling of hybrid electric vehicles and the Ph.D. degree in multiscale modeling of micro and nanoscale thin films from the Ohio State University, Columbus OH, USA, in 2002 and 2008, respectively.

From 2008 to 2012, he was a Postdoctoral Researcher with Purdue University, West Lafayette, IN, USA, and with Northwestern University, Evanston, IL, USA. He is currently an Assistant Professor with the Department of Mechanical and Civil Engineering, Purdue University Northwest, Hammond, IN. His research focuses on multiscale modeling and characterization of advanced nano/bio/energy systems and materials. The scope of his multiscale modeling and characterization ranges from atomistic to macro scales utilizing both theoretical and experimental studies.

Dr. Kim is a member of IEEE, ASME, and TMS.



Benjamin G. Wojkovich received the B.Sc. degree in physics and the second B.Sc. degree in mechanical engineering, both from Purdue Northwest, Hammond, IN, USA, in 2008 and 2017, respectively.

His research interest includes renewable energy.